# A Statistical–Topographic Model for Mapping Climatological Precipitation over Mountainous Terrain

CHRISTOPHER DALY

*Oregon State University, Corvallis, Oregon*

RONALD P. NEILSON

*USDA Forest Service, Corvallis, Oregon*

DONALD L. PHILLIPS

*U.S. Environmental Protection Agency, Corvallis, Oregon*

(Manuscript received 18 September 1992, in final form 31 July 1993)

ABSTRACT

The demand for climatological precipitation fields on a regular grid is growing dramatically as ecological and hydrological models become increasingly linked to geographic information systems that spatially represent and manipulate model output. This paper presents an analytical model that distributes point measurements of monthly and annual precipitation to regularly spaced grid cells in midlatitude regions. PRISM (Precipitation–elevation Regressions on Independent Slopes Model) brings a combination of climatological and statistical concepts to the analysis of orographic precipitation. Specifically, PRISM 1) uses a digital elevation model (DEM) to estimate the "orographic" elevations of precipitation stations; 2) uses the DEM and a windowing technique to group stations onto individual topographic facets; 3) estimates precipitation at a DEM grid cell through a regression of precipitation versus DEM elevation developed from stations on the cell's topographic facet; and 4) when possible, calculates a prediction interval for the estimate, which is an approximation of the uncertainty involved. PRISM exhibited the lowest cross-validation bias and absolute error when compared to kriging, detrended kriging, and cokriging in the Willamette River basin, Oregon. PRISM was also applied to northern Oregon and to the entire western United States; detrended kriging and cokriging could not be used, because there was no overall relationship between elevation and precipitation. Cross-validation errors in these applications were confined to relatively low levels because PRISM continually adjusts its frame of reference by using localized precipitation–DEM elevation relationships.

## 1. Introduction

Estimates of the amount and spatial distribution of monthly and annual precipitation are critical inputs to a variety of ecological and hydrological models. These include vegetation models, water balance models, water quality models, and crop production models (e.g., Running et al. 1987; Dolph et al. 1992). The demand for precipitation fields on a regular grid is growing dramatically as models become increasingly linked to geographic information systems (GIS) that spatially represent and manipulate model output. However, lack of data and of a conceptual framework for mapping orographic precipitation has hindered the development of precipitation grids for complex terrain.

The purpose of this study was to develop a method for distributing point measurements of monthly and annual average precipitation to regularly spaced grid cells at regional to continental scales. The result was an objective precipitation distribution model called PRISM (Precipitation–elevation Regressions on Independent Slopes Model). PRISM is well suited to regions with mountainous terrain because it incorporates a conceptual framework that addresses the spatial scale and pattern of orographic precipitation. This paper describes the PRISM modeling system and compares its advantages and limitations to those of three commonly used geostatistical methods: ordinary kriging, elevationally detrended kriging, and elevational cokriging.

## 2. Methods for estimating areal precipitation

Historically, most methods for estimating areal and gridded precipitation from point data have fallen into three major groups: graphical, topographical, and numerical. Graphical methods involve mapping of precipitation data, sometimes in combination with precipitation–elevation analyses, and include isohyet

*Corresponding author address:* Christopher Daly, U.S. EPA Environmental Research Laboratory, 200 S.W. 35th Street, Corvallis, OR 97333.

mapping (Reed and Kincer 1917; Peck and Brown 1962) and Thiessen polygon estimation (Thiessen 1911). Topographical methods involve the correlation of point precipitation data with an array of topographic and synoptic parameters such as slope, exposure, elevation, location of barriers, and wind speed and direction (Spreen 1947; Burns 1953; Schermerhorn 1967; Houghton 1979).

Over the past decade, the most commonly used precipitation distribution methods have been numerical. These are interpolation procedures in which a numerical function, developed or prescribed, is used to weight irregularly spaced point data to estimate a regularly spaced prediction grid.[1] Inverse-distance weighting is an example of a simple numerical interpolation method. In this case, the weighting of the data points is prescribed to decrease as the distance between the points increases. Kriging is a geostatistical approach (Matheron 1971) that has gained acceptance as a tool for the interpolation of many types of data, including precipitation (Chua and Bras 1982; Dingman et al. 1988; Phillips et al. 1992). In kriging, a semivariogram model that best fits the data is developed to arrive at optimum station weights for interpolation. A potential drawback of kriging is that it implicitly relies on the data to directly represent the spatial variability of the actual precipitation field. If the data are not representative (as is often the case in complex terrain), the accuracy of the resulting interpolated field will be in question. In addition, more than one semivariogram may be needed to estimate precipitation at various time periods for which the processes producing the precipitation patterns differ. For example, a semivariogram used in January may not be applicable to July, because of seasonal differences in precipitation processes.

Recently, elevationally detrended kriging and cokriging with elevation as a covariate have been used to bring topographic influences into the calculations (Phillips et al. 1992; Hevesi et al. 1992a,b). The resulting precipitation fields often show more topographically related spatial patterns in complex terrain than those from ordinary kriging. However, application is limited to areas characterized by a strong, overall precipitation–elevation relationship (i.e., regions dominated by one main orographic regime).

Attempts are now being made to use digital elevation models (DEMs), sometimes in conjunction with orographic models, to predict the physical influences of topographic factors on precipitation patterns (e.g., Peck and Schaake 1990; Fan and Duffy 1991; Hay et al. 1991). Such approaches are promising because they stress the physical nature of orographic influences on precipitation. As will be seen in the next section, the PRISM modeling system incorporates some general aspects of the physical approach while retaining the analytical nature of the numerical approaches.

## 3. The PRISM conceptual framework

PRISM incorporates a conceptual framework that addresses orographic scale and pattern across the landscape. Below we introduce and discuss the three main aspects of this framework: 1) the effects of elevation on precipitation, 2) the spatial scales at which orographic effects are observed, and 3) the spatial patterns of orographic regimes over complex terrain.

### *a. Precipitation–elevation relationships*

On a given mountain slope, climatological precipitation typically increases with elevation (Alter 1919; Barrows 1933; Spreen 1947; Schermerhorn 1967; Hibbert 1977; Smith 1979). This phenomenon, commonly called the orographic effect, is evident worldwide (e.g., Henry 1919; Hutchinson 1968; Vuglinski 1972). Depending on its size and orientation, a mountain or range of mountains can increase the intensity of cyclonic precipitation by retarding the rate of movement of the storm and causing forced uplift of the air mass (Barry and Chorley 1976; Marwitz 1987). In summer, the orographic effect may trigger a conditional or convective instability in an otherwise stable air mass, producing a local redistribution of precipitation over the higher ground.

Local increases in precipitation with elevation approximate a linear form in many regions. Examples include Arizona (Hibbert 1977; Osborn 1984), Nevada (Houghton 1979), Idaho (Hanson et al. 1980), the Great Smoky Mountains (Donley and Mitchell 1939), New England (Barrows 1933), Utah (Alter 1919; Lull and Ellison 1950; Peck and Brown 1962), the southern Rocky Mountains (Hart 1937), and southern California (Burns 1953). Under some conditions the relationship between precipitation and elevation may be best described by log-linear or exponential functions, but the simple linear form is easy to use and appears to be an acceptable approximation in most situations.

In subtropical regions, limited vertical cloud development causes the precipitation maximum to occur below the crests of higher mountains (e.g., the Hawaiian islands). In contrast, the climatological precipitation maximum at midlatitudes usually occurs at or near the crest of the topographic barrier (e.g., Lull and Ellison 1950; Barry 1973; Hanson et al. 1980). There are exceptions, however. In large-scale precipitation situations, a spatial displacement of the precipitation maximum upwind of the crest may occur over very broad barriers as a result of lifting and condensation

[1] In this paper, *grid* refers to a two-dimensional array of regularly spaced grid cells. A *grid cell* refers to a single pixel that has dimensions equivalent to the resolution of the grid. For example, each cell in a 1-km resolution grid is 1 km × 1 km in size. A value assigned to a pixel, such as a precipitation estimate, is positioned at the cell center. However, it is not a point value; rather, it represents an average value over the entire cell.

in the upstream flow before the barrier is reached (Smith 1979). This phenomenon appears to be partially responsible for an annual precipitation maximum windward of the crest of the northern Sierra Nevada of California (e.g., Varney 1920; Lee 1941; Armstrong and Stidd 1967), where the horizontal distance from windward base to crest is about 120 km. Although not well documented, in very high mountains an upwind displacement of the precipitation maximum could theoretically be produced by a "drying out" of the ascending air due to upstream rainout. Over barriers with steep, narrow upwind faces, the delay between the condensation and precipitation maxima (due to hydrometeor formation and fall) (Smith 1979) and airflow acceleration over the crest may displace the precipitation maximum to the lee side of the crest. This is reflected in long-term precipitation observations on steep, windy ridges in southwestern Idaho where the horizontal distance from windward base to crest is less than 10 km (Johnson and Hanson, USDA Agricultural Research Service 1993, personal communication).

The magnitude of displacement (if any) in the precipitation maximum from a mountain crest is not easily generalized for mapping purposes, and depends on moisture source, barrier characteristics, storm type, wind speed, and other factors. Even when available, raingage data themselves may not present a true picture of precipitation distribution near mountain crests. It is clear that undercatch of precipitation, especially snow, can be significant (Gjorsvik 1972; Rechard 1972; Sevruk 1974; Rodda and Smith 1986). The present version of PRISM assumes that precipitation on a given slope increases with elevation to a maximum at the mountain crests, unless local station data dictate otherwise. As such, this configuration is suitable primarily to midlatitude regions (or lower mountains in other regions), and may spatially offset or perhaps overestimate the "actual" precipitation maximum in some instances.

### b. *The spatial scale of orographic effects*

The scale at which orographic effects are observed is of great importance to this analysis, because of our desire to use a DEM as a GIS-compatible source of spatially gridded elevation data. There is an implicit mismatch in scale when one uses relationships between station point elevations and precipitation to estimate precipitation at DEM grid cells. The elevation at the center of a DEM grid cell does not represent the elevation at that point, but reflects an average or otherwise smoothed elevation representing the entire grid cell. Hence, the DEM cell elevation will rarely match the station elevation, even if the station is at the exact center of the grid cell. Generally, the finer the resolution of the DEM, the more closely the elevation of the grid cell will match that of the point. But limited computing resources and a lack of widespread fine-resolution coverage often limit the resolution of DEMs used in regional applications to a range of about 1–10 km. To maintain a consistent scale and avoid mismatches between station point and DEM grid-cell elevations, PRISM calculates elevations of the stations from their positions on the DEM.

Two questions immediately arise: how does the DEM grid resolution compare to the scale of the orographic effects we are attempting to simulate, and is there an "optimal" resolution for orographic effects? A definitive answer is not available, but there is evidence to suggest that relatively coarse grid-scale DEMs may actually give excellent estimates of the "orographic" elevations of stations in many instances. Several researchers have found that broad-scale topographic features at scales of 2–15 km were more highly correlated with precipitation than point-based topographic features (Spreen 1947; Burns 1953; Schermerhorn 1967; Hibbert 1977). Experiments with a 5-min latitude–longitude (approximately 6 km × 9 km) DEM (National Geophysical Data Center 1989) suggest that in many regions the elevations of the DEM can offer a better approximation of a station's orographic elevation than the station's actual elevation. Figure 1 illustrates relationships between precipitation and elevation for four stations in the Columbia River gorge, a deep but narrow river valley bisecting the Cascade Range and forming the border between Washington and Oregon. The Cascades are a significant orographic feature oriented normal to the prevailing westerly wind flow. Moist air masses are lifted by the large-scale bulk of the mountains on either side of the gorge, causing relatively high amounts of precipitation to fall within the gorge. Consequently, elevations at 5-min resolution,

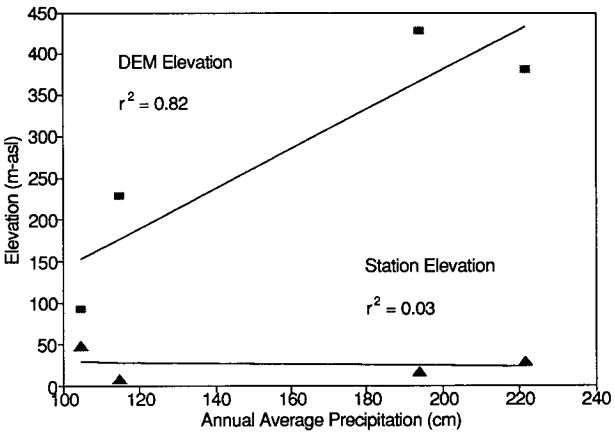


FIG. 1. Relationships between measured annual precipitation and two elevation parameters (actual station elevation and the 5-min DEM elevation) at the station location in the Columbia River gorge. Triangles denote actual station elevation points and rectangles denote DEM elevation points. The relationship using the DEM elevation is much more useful because its 5-min resolution better approximates the scale of orographic processes illustrated in the data. All stations shown are located west of the Cascade Range crest.

which do not resolve the gorge well, are much more highly correlated with precipitation than the station elevations.

Of course, there are many complicating factors. The orographic scale undoubtedly depends on the scale of the prevailing storm type—large-scale frontal systems have inherently larger scales than localized convective cells. The orographic scale illustrated in the data may also depend on the relationship between the scale of the topographic features involved and the density and placement of the data points. In the Columbia Gorge example, the 5-min DEM approximated the orographic scale associated with the Cascade Mountain barrier. However, there are undoubtedly smaller-scale orographic effects imbedded in this larger scale effect that would produce an increase in precipitation from, say, the bottom of the gorge to the rim. However, there are no stations at various heights above the floor of the gorge to illustrate this. In essence, we have only enough stations to resolve orographic effects at the scale of the Cascade Mountains; levels of the orographic "hierarchy" operating at finer scales cannot be resolved readily. The best DEM resolution therefore becomes more a function of data density than of the actual scale of orographic effects. Another potential factor is the temporal resolution of the data. Small-scale orographic effects may be more likely to be resolved in short-time-interval data than in data averaged over a long time period.

Data from the Reynolds Creek watershed (Hanson et al. 1980), one of the densest precipitation networks in the country, gives some insight into the minimum orographic scale in southwestern Idaho. These data indicate that mountain ridges 8 km apart experience slight but distinct dry and wet exposures during winter. A DEM with a cell size of no more than 2 km would probably be needed to resolve these orographic effects. Other examples of small-scale precipitation variations include the enhancement of precipitation over low hills in Illinois (Changnon et al. 1975) and Sweden (Bergeron 1968), and precipitation deficits in deep, narrow valleys in Canada (Longley 1975).

We have chosen to start with a 5-min DEM resolution for this analysis, because it appears to approximate the scale of orographic effects that can be readily explained by routinely available data in regional applications. The relationship between the scale of topographic features, data density, temporal resolution, and optimum DEM resolution will be a major focus of further research with PRISM (see section 6).

### c. *The spatial patterns of orographic regimes*

The characteristics of the relationship between measured precipitation and elevation can vary appreciably from hillslope to hillslope, and are influenced by differences in steepness of the terrain, upwind barriers, and slope orientation, among other factors. This can make it difficult to obtain a usable relationship between elevation and precipitation, unless rainfall stations are grouped into regions that control for such factors. Numerous topographic station groupings resulting in strengthened precipitation–elevation relationships have been documented (Alter 1919; Barrows 1933; Hart 1937; Donley and Mitchell 1939; Lull and Ellison 1950; Burns 1953; Peck 1962; Houghton 1979; Hanson et al. 1980; Osborn 1984).

To effectively model the spatial pattern of orographic precipitation in complex terrain, it is essential that topographic regions be recognized and isolated. To this end, a mountainous landscape can be divided into a mosaic of topographic faces, or "facets," each assumed to experience a different orographic regime. Each topographic facet is a contiguous area over which the slope orientation is reasonably constant. For example, the western slope of the Oregon Cascades represents a large, west-facing topographic facet (see section 4c). Topographic facets are best delineated by using a DEM with a resolution that closely matches the smallest orographic scale supported by the data, thereby reducing the number of facets delineated at terrain scales too small to be resolved by the data and avoiding overaggregation of orographically important facets.

## 4. Description of the model

### a. *Overview*

In operation, PRISM 1) estimates the "orographic" elevation of each precipitation station using a DEM at 5-min latitude–longitude grid spacing, and 2) assigns each DEM grid cell to a topographic facet by assessing slope orientation. PRISM then estimates precipitation at each DEM cell by 3) using a windowing technique to develop a precipitation–DEM elevation regression function from nearby rainfall stations on the cell's facet; and 4) predicting precipitation at the cell's DEM elevation with this regression function. Whenever possible, PRISM calculates a prediction interval for the estimate, which is an approximation of the uncertainty involved.

By using many precipitation–DEM elevation relationships developed within local windows and on individual topographic facets, rather than a single domainwide relationship, PRISM continually adjusts its frame of reference to accommodate local and regional changes in orographic regime.

### b. *PRISM structure and function*

The overall structure of the PRISM system is shown in Fig. 2. The system consists of three functional components: FACET, which generates grids of topographic facets from the DEM; PRISM, which assimilates the DEM, the facet grids, and station data to produce the estimated precipitation and prediction interval grids; and GRADIENT, a postprocessor to these grids. The PRISM system requires several input parameters, most

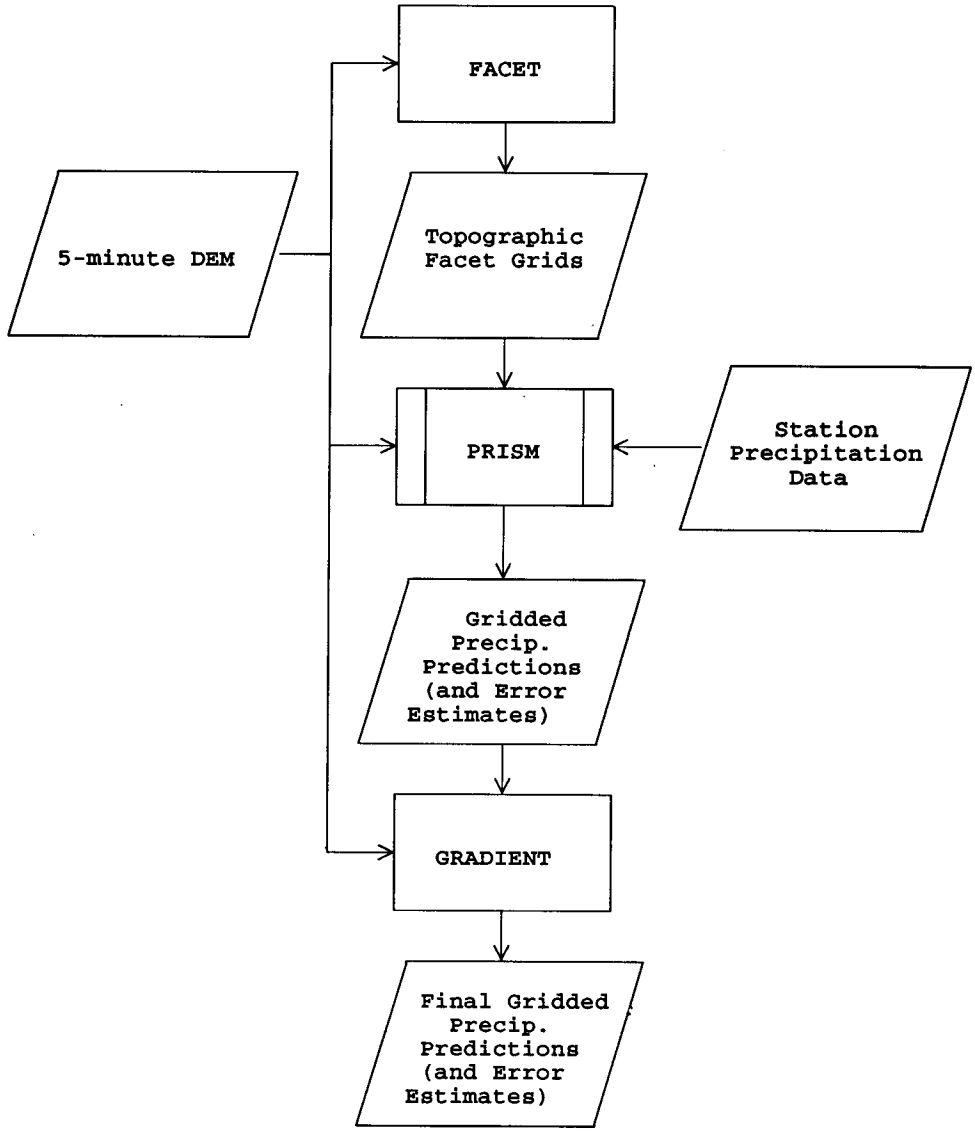


FIG. 2. Overall structure of the PRISM modeling system.

of which can be determined objectively or left as default values. PSTAT, a statistical version of PRISM, is used to determine the optimum values of the most important input parameters (see section 5 for further discussion). Parameter definitions and methods of determination are listed in Table 1.

*c. FACET*

As discussed in section 3, each topographic facet is a contiguous area over which the slope orientation is reasonably constant. FACET assigns a slope orientation to each DEM cell at column $i$, row $j$ by first calculating elevation gradients across the cell from west to east and south to north. Assuming Cartesian coordinates, the west–east gradient is calculated as the difference in elevation between the adjacent cell $(i - 1, j)$ to the west and the adjacent cell $(i + 1, j)$ to the east. The south–north gradient is calculated as the difference in elevation between the adjacent cell $(i, j - 1)$ to the south and the adjacent cell $(i, j + 1)$ to the north. The slope is judged to be flat if neither the west-to-east nor the south-to-north gradients are equal to or greater than a prescribed gradient (MINSTP; Table 1). If the slope is not flat, the cell is categorized as facing north, south, east, or west.

In practice, the definition of a topographic facet in PRISM depends largely on the availability of data points to describe the precipitation–DEM elevation regression function on that facet. In many cases the number of data points on a facet is very small. There-

TABLE 1. Input parameters required by the PRISM system. Range, default, and comments on estimation method assume model is being applied to a DEM with 5-min latitude–longitude resolution.

| Parameter | Definition | Units | Modeling system component | Range and default value | Method for estimation |
|---|---|---|---|---|---|
| MINSTP | Elevation gradient below which terrain is assumed to be flat | meters per grid cell | FACET | 1–25<br>15 | 15 is used for most applications |
| MAXRAD | Maximum radius within which station search will be conducted | grid cells | PRISM | 2–10<br>none | Cross validation (PSTAT) |
| MINRAD | Minimum radius within which all stations are included | grid cells | PRISM | 2–5<br>none | Cross validation (PSTAT) |
| MINSTA | Minimum number of stations required for cell $P/E$* regression calculation | stations | PRISM | 3–10<br>none | Cross validation (PSTAT) |
| B1MIN | Minimum allowable slope for cell $P/E$ regression function | per kilometer | PRISM | 0.0 | 0.0 is used for most applications |
| B1MAX | Maximum allowable slope for cell $P/E$ regression function | per kilometer | PRISM | 2.0–3.0<br>3.0 | Largest $P/E$ slope expected on a single facet in the domain |
| DB1 | Default slope for cell $P/E$ regression function | per kilometer | PRISM | 0.6–1.3<br>none | Mean slope from all valid regressions in domain |
| B1EX | Extrapolation slope for cell $P/E$ regression function | per kilometer | PRISM | 1.5–2.5<br>2.0 | Hold back high-elevation data and find B1EX giving best prediction stats |
| B1MAXG | Maximum allowable slope for a $P/E$ relationship between cells | per kilometer | GRADIENT | 2.5–5.0<br>4.0 | The largest $P/E$ slope expected between facets in the domain |
| MINSLP | Minimum elevation gradient needed to invoke GRADIENT operation | Meters per grid cell | GRADIENT | 75–150<br>100 | 100 appears to be good for United States |

* Precipitation–DEM elevation.

fore, there must be a mechanism by which the spatial extent of a facet can be dynamically broadened to encompass more data points if needed. This is done by subjecting the DEM to a standard five-point filter, in which the cell elevation $E_{ij}$ is computed as

$$E_{ij} = 0.5E_{ij} + 0.125(E_{i+1j} + E_{i-1j} + E_{ij+1} + E_{ij-1}). \quad (1)$$

To accommodate a large range of potential data point densities, FACET computes six different facet grids: 1) facet grid is derived from the unfiltered DEM, 2) the DEM is subjected to 8 filtering passes, 3) 16 passes, 4) 24 passes, 5) 32 passes, and 6) 40 passes. A 5-min DEM subjected to more than 40 filtering passes does not resolve some of the major orographic features that exist in the United States. Facets that are only a single cell in width are assimilated into the surrounding facets, because at least two grid cells are needed on a facet to give some elevational variation for the regression calculations. Narrow facets that straddle the crests of mountains (and thus show a net slope that is flat), undergo a special assimilation process. The precipitation regime on mountain crests is usually more similar to that of the windward side than the leeward side. At midlatitudes the windward sides of north–south- and west–east-oriented mountain ranges are typically the west and south slopes, respectively. Thus, ridge–crest facets on approximately north–south ranges are assimilated into the adjacent facet to the west and those on approximately east–west ranges are assimilated into the adjacent facet to the south. This configuration can be altered easily for regions exhibiting different climatological characteristics.

Figure 3 illustrates outputs from FACET for northwestern Oregon on the unfiltered 5-min DEM and on the same DEM after 40 filtering passes. The unfiltered

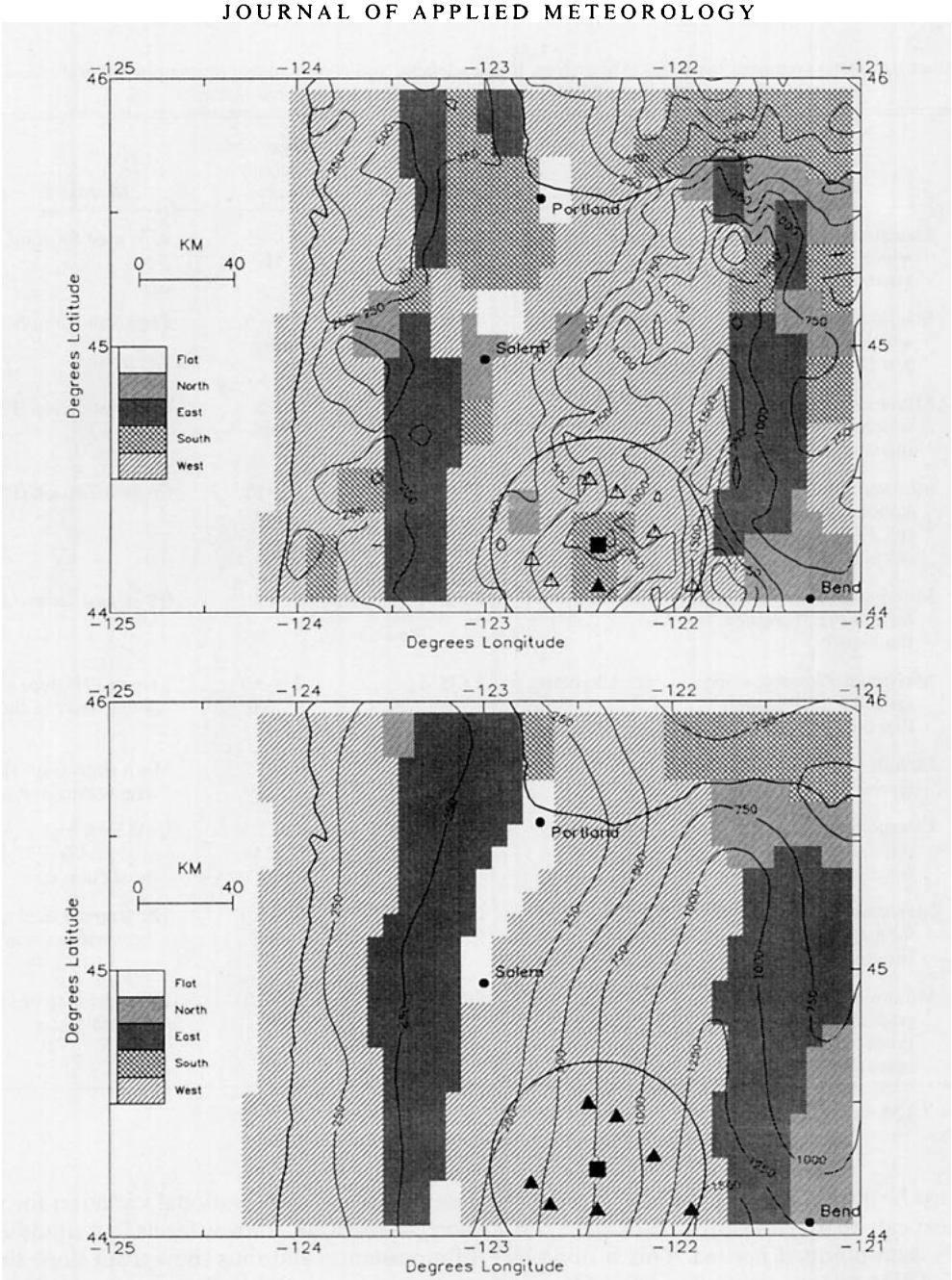


FIG. 3. Northwestern Oregon topographic facets produced by FACET and an example search window used by PRISM for (a) the unfiltered DEM and (b) the DEM filtered 40 times. Solid square denotes an example grid cell for which precipitation is to be estimated by PRISM. Open triangles are stations that fall within the grid cell's window but are rejected because they lie on a different topographic facet. Solid triangles are stations accepted for developing the precipitation–DEM elevation regression function for the grid cell.

DEM (Fig. 3a) resolves a detailed array of facets, some of which are quite small. The highly filtered DEM (Fig. 3b) resolves only the gross terrain features, and produces a smaller number of larger facets.

### *d. PRISM*

The structure of the main PRISM model is detailed in Fig. 4. "Orographic" elevations for each precipitation station are derived from the 5-min DEM by 1) locating the DEM grid cell center that falls nearest to the station location; 2) finding the four surrounding grid cells adjacent to the cell in step 1; and 3) calculating a weighted mean elevation of these five DEM cells, with each cell weighted inversely by its center's distance from the station location. For each grid cell on the DEM, PRISM retrieves the appropriate stations, develops a precipi-

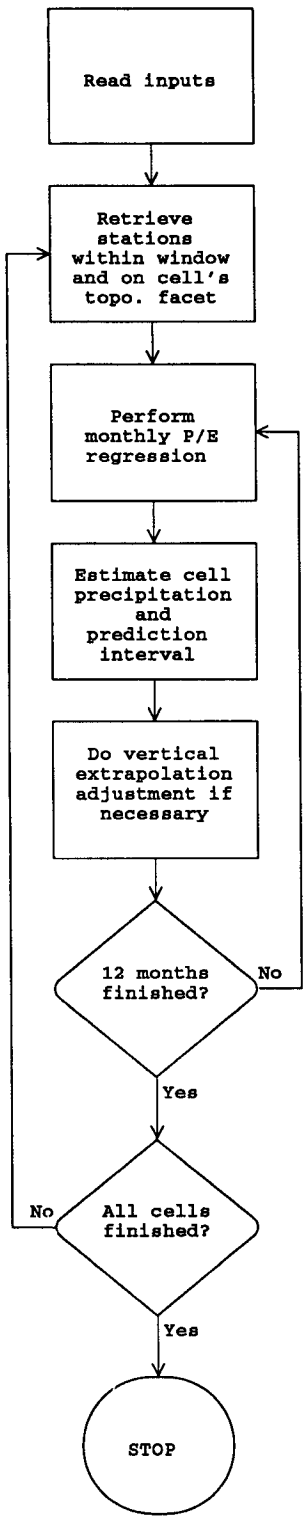


FIG. 4. Process flow for monthly operation of the main PRISM model.

tation–DEM elevation regression function, estimates precipitation at the cell, and, if necessary, makes vertical extrapolation adjustments to the estimate. PRISM then estimates the uncertainty in the estimate by calculating a regression prediction interval. Each of these processes is discussed in detail below.

### 1) STATION RETRIEVAL

All stations located within a prescribed maximum radius (MAXRAD; Table 1) from the DEM grid cell are retrieved. Those stations not falling on the cell's topographic facet are omitted (Fig. 3). If the number of remaining stations is less than a prescribed minimum number (MINSTA; Table 1), PRISM attempts to include more stations by using a filtered FACET grid. PRISM starts with the FACET grid with eight filtering passes, adding any stations that now fall on the same facet as the DEM grid cell. This process continues with more highly filtered FACET grids until MINSTA (Table 1) is reached or the most highly filtered FACET grid has been used, whichever comes first. If the number of stations on the correct facet exceeds MINSTA on the first try (using the unsmoothed FACET grid), all stations within a prescribed minimum radius (MINRAD; Table 1) and on the same facet are accepted. Conversely, if no stations on the same facet are available even at the highest smoothing level, the one station that is nearest to the DEM grid cell, regardless of facet, is selected for use in the regression calculations.

Stations located on cells that have the same orientation (i.e., north, south, east, or west) as the DEM grid cell but lie on a completely separate facet are eliminated from the search. For example, a station located on the western slope of the Oregon Coast Range is not used in defining the precipitation–DEM elevation function for the western slope of the Cascades (see Fig. 3).

An example of the station search process is shown in Fig. 3. The grid cell to be estimated is on a small south-facing facet. On the unsmoothed FACET grid there is only one station on this facet—not enough to develop a precipitation–DEM elevation relationship (Fig. 3a). PRISM searches successively smoother FACET grids until enough stations are accumulated. After 40 filtering passes, local variations in topography have been minimized, allowing surrounding stations to be accepted into the regression calculation (Fig. 3b).

### 2) DEVELOPMENT OF PRECIPITATION–DEM ELEVATION REGRESSION FUNCTIONS

Monthly and annual linear precipitation–DEM elevation regression functions are generated from the station dataset retrieved for the grid cell. If the slope of a calculated regression line falls outside prescribed bounds (B1MIN and B1MAX; Table 1), the model

attempts to find an influential outlying station that is causing the unusual slope. The most influential outlier is defined using two criteria. Upon deletion, it produces: 1) the largest change in the slope of the regression line, and 2) a new regression slope that falls between B1MIN and B1MAX. If an influential outlier is found, it is deleted from the regression calculation. If no single outlier can be deleted to bring the slope to within allowable limits, the slope is set to a prescribed default value (DB1; Table 1). If only one station is in the regression dataset, the default slope DB1 (Table 1) is invoked immediately.

B1MIN, B1MAX, and DB1 are not expressed in absolute units (such as centimeters of precipitation per kilometer of elevation), which vary greatly temporally as well as spatially. Rather, each of these regression slopes, which we will collectively call B1, is expressed as a proportion of the average precipitation of the regression dataset for each cell $(i, j)$:

$$B_1 = \frac{b_{1_{ij}}}{\overline{P_{ij}}},$$

where

$$\overline{P_{ij}} = \frac{1}{n_{ij}} \sum_{k=1}^{n_{ij}} P_{k_{ij}}; \qquad (2)$$

$b_{1_{ij}}$ is the precipitation–DEM elevation regression slope for the cell, $P_{k_{ij}}$ is the $k$th precipitation data point in the regression dataset for the cell, and $n_{ij}$ is the number of stations used in the regression calculation for the cell. Evidence gathered during model development indicates that this method of expression is relatively stable in both space and time. In PRISM applications to Colorado, California, Arizona, and the Pacific Northwest, the domain-mean precipitation–DEM elevation slope varied from 25.3 cm km$^{-1}$ in low-precipitation domains to 217.1 cm km$^{-1}$ in high-precipitation regions. When the domain-mean slope was expressed in the form of (2), the range was only 0.90–1.28 km$^{-1}$.

B1MIN is set to zero in most applications, because precipitation should theoretically increase with elevation on a single topographic facet (although this may not always be the case when facets are smoothed to compensate for sparse data). A default value for B1MAX was found by analyzing monthly precipitation data from stations on the leeward sides of major mountain ranges in the United States, where precipitation gradients are greatest. The maximum value observed was 3.0 km$^{-1}$, the gradient between Three Sisters and Santiam Pass, Oregon.

### 3) Precipitation estimation

A monthly or annual precipitation prediction at grid cell $(i, j)$ is calculated as

$$P_{ij} = b_{0_{ij}} + b_{1_{ij}} E_{ij}, \qquad (3)$$

where $b_{1_{ij}}$ and $b_{0_{ij}}$ are, respectively, the monthly regression slopes and intercepts for the cell, and $E_{ij}$ is the DEM elevation of the cell. Any $P_{ij}$ less than zero is set to zero.

### 4) Vertical extrapolation adjustment for coarse-grid simulations

PRISM presently operates on a 5-min latitude–longitude DEM, which represents the terrain in a smoothed, simplified fashion. Unfortunately, the smoothing effect can significantly reduce the height of relatively narrow or isolated mountains and ridges. This is most apparent in regions where the terrain alternates between flat valleys and towering, sharply defined peaks (e.g., the intermountain west). The precipitation–DEM elevation function is often developed from sites located only on lower, gentle slopes, which are represented reasonably well by the coarse-grid DEM. Extrapolation of the regression line up a sharply defined ridge, however, can lead to an underestimation of precipitation on the ridge, because the DEM may not resolve such localized elevational gradients.

We have implemented a temporary algorithm to adjust precipitation estimates for locally high elevations that have been reduced by the coarse-grid DEM, when 1) the elevational range of the stations used in the precipitation–DEM elevation function is small (less than 1000 m) and 2) upward extrapolation of the function is necessary to estimate precipitation. This is done by allowing the slope of the precipitation–DEM elevation function to be changed to a prescribed value (B1EX; Table 1) above the elevation of the highest station in the regression dataset for cell $(i, j)$. The new function with slope B1EX begins on the old regression line at the elevation of the highest station. B1EX is expressed as a fraction of the precipitation per kilometer of elevation at the point where the new line begins. A reasonable value for B1EX was estimated by holding back high-elevation SNOTEL (snow telemetry) precipitation data (USDA Soil Conservation Service 1988) in the intermountain region and finding the B1EX that provided estimates of the SNOTEL data with the least overall error and bias in repeated applications. These tests showed that a B1EX of 2.0 gave consistently good results. In the future, we hope to minimize or eliminate the need for this adjustment by developing more sophisticated versions of PRISM that will run on finer-resolution DEMs within the confines of the available data density (see section 3b for discussion of data density).

### 5) Estimation of prediction intervals

To address the degree of uncertainty in the estimated precipitation values, PRISM calculates 95% prediction intervals. Since PRISM currently uses linear regression to estimate precipitation as a function of elevation,

standard methods for calculation of prediction intervals for the dependent variable ($Y$) are used. These prediction intervals take into account both the variation in the possible location of the expected value of $Y$ for a given $X$ (since the regression parameters must be estimated), and variation of individual values of $Y$ around the expected value (Neter et al. 1989). The formula used for calculating the variance of $Y$ (precipitation) for a given value of $X = X_h$ (elevation) is

$$s^2(Y_h) = s^2(\hat{Y}_h) + \text{MSE}$$

$$= \text{MSE}\left[1 + \frac{1}{n} + \frac{(X_h - \bar{X})^2}{\sum_{i=1}^{n} (X_i - \bar{X})^2}\right], \quad (4)$$

where $s^2(Y_h)$ is the estimated variance of the expected value of $Y_h$ at $X = X_h$, MSE is the regression mean-square error, and $n$ is the number of points in the regression (Neter et al. 1989). The 95% prediction intervals were created as

$$\hat{Y}_h \pm t_{0.975,\text{df}} s(\hat{Y}_h), \quad (5)$$

where $t_{0.975,\text{df}}$ is the 97.5 percentile value of the $t$ distribution with df degrees of freedom for MSE. Calculation of these estimation variances and prediction intervals are not possible when either 1) fewer than three data points are available for regression in a window; 2) the regression slope does not fall between B1MIN and B1MAX and the domain-mean precipitation–DEM elevation slope is substituted; 3) the estimated precipitation value undergoes vertical extrapolation adjustment; or 4) the estimated precipitation value is modified by the GRADIENT postprocessor (see section 4e).

Kriging and cokriging estimation variances assume the correctness of the semivariogram and cross-semivariogram models, and do not incorporate any uncertainty related to model "goodness of fit." The method outlined above for calculating estimation variances in PRISM does include this source of variability. Estimation variance tends to be higher with fewer regression points, greater scatter around the regression line, or elevations further away from the mean regression elevation. On the other hand, kriging and cokriging variances incorporate the spatial proximity of the estimated point to the surrounding data points used in the interpolation. The closer the supporting data points, the lower the estimation variances are in kriging and cokriging. PRISM does not explicitly incorporate the spatial proximity of surrounding data points in its calculation of estimation variance. However, the restriction of the interpolation to a small window on a particular topographic facet is an attempt to control other factors affecting precipitation besides elevation. The assumption is made that the regression relationship developed for that facet and window applies equally well to all points within that facet and window, regardless of their spatial relationship to the particular supporting data points.

### *e. Gradient*

GRADIENT is a postprocessor to the PRISM estimated precipitation grids. GRADIENT does between-cell precipitation–DEM elevation slope checking (as was done in the main PRISM model for cell regression functions), primarily to avoid overly sharp discontinuities in predictions between adjacent topographic facets. For instance, the precipitation regime between the windward and leeward slopes of the Cascades is sharply pronounced. This may result in a spatial discontinuity, or step change, in predictions between adjacent cells if insufficient data are available to adequately define the sharp gradient.

The prescribed maximum precipitation–DEM elevation slope, B1MAXG (Table 1), is set to a somewhat higher value in GRADIENT than its counterpart (B1MAX) in the main model because steep precipitation–DEM elevation slopes are to be expected between some adjacent facets. No minimum slope is specified because very large negative slopes are common between sharply defined facets. GRADIENT ignores areas of flat terrain (which are typically within a single facet) by applying a minimum elevation gradient criterion (MINSLP; Table 1).

GRADIENT searches for discontinuities on a cell-by-cell basis. When the precipitation–DEM elevation slope between two adjacent cells exceeds B1MAXG and the elevation gradient between the cells exceeds MINSLP, the lower precipitation value of the two cells is increased until the slope is decreased to B1MAXG. In practice, the primary effect of GRADIENT is a "feathering out" of any sharp discontinuities in the precipitation fields on the leeward sides of large mountain ranges.

## 5. Model evaluation

The performance of PRISM was compared to those of geostatistical interpolation methods through application to the Willamette River basin, Oregon. This afforded the opportunity to evaluate PRISM alongside three types of geostatistical methods compared in Phillips et al. (1992): kriging, detrended kriging, and cokriging. For more rigorous testing, PRISM was also applied to northern Oregon and to the entire western United States. Detrended kriging and cokriging could not be applied to these regions of such widely varying orographic regimes.

### *a. Willamette River basin*

The Willamette River basin (Fig. 5) is bounded by the Coast Range on the west, Cascade Range on the east, and the Columbia River on the north. Elevations within the basin range from near sea level at Portland

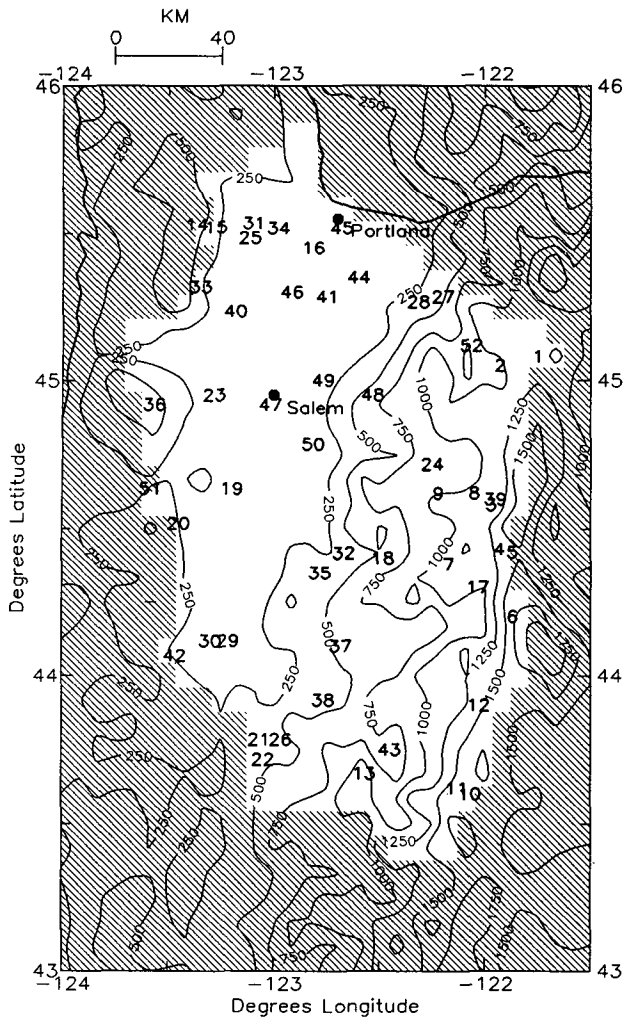


FIG. 5. The Willamette River basin modeling domain. Elevation contour interval is 250 m. Numbers 1–15 denote SNOTEL sites, and 16–52 denote NWS and cooperator stations.

to over 3200 m (1750 m on the 5-min DEM in Fig. 5) in the high Cascades. Measured annual precipitation ranges from about 100 cm in the Willamette Valley to nearly 300 cm in the Coast Range west of Salem. The best available isohyetal map for Oregon (USDA Soil Conservation Service 1964) had estimates in excess of 500 cm for a few locations in the Coast Range. Most precipitation in the basin is produced by cyclonic storms that push onshore from the Pacific Ocean during the fall, winter, and spring. Rainfall is greatest on the western side of the Coast Range, and drops off rapidly on the eastern side into the somewhat drier Willamette Valley. Precipitation increases gradually up the western slope of the Cascades, reaching levels that approach those of the Coast Range in some locations. Summer precipitation is usually very light, with only minor convective activity in the high mountains and occasional weak cyclonic storms.

The precipitation dataset was that used by Phillips et al. (1992). The dataset consisted of average annual precipitation for the period 1982–88 at 52 stations (Fig. 5). Thirty-seven stations were operated by the National Weather Service and cooperators (EarthInfo 1990) and 15 were Soil Conservation Service SNOTEL stations (USDA Soil Conservation Service 1988). A 5-min latitude–longitude DEM grid provided elevation data for 478 cells within the basin (National Geophysical Data Center 1989). Kriging, elevationally detrended kriging, and elevational cokriging were applied to the study area by Phillips et al. (1992). Kriging involved a procedure of selecting and iteratively refining a semivariogram model for log annual precipitation. The final model exhibited the lowest reduced-mean and reduced-variance cross-validation statistics (Yates and Warrick 1987). Cross validation was done using the "jackknife" procedure—station precipitation values were deleted one at a time, and new values estimated by kriging.

For elevationally detrended kriging, a basinwide linear regression was performed with log annual precipitation as the dependent variable and log elevation as the independent variable. The log annual precipitation residuals from the regression were used to construct a semivariogram. As in kriging, the model was refined iteratively using cross validation. Cokriging required a semivariogram for log elevation, a cross semivariogram for the interaction of log annual precipitation and log elevation, as well as the log annual precipitation semivariogram (developed for kriging). The log elevation semivariogram used the 478 5-min DEM elevations plus the 52 weather station elevations. Precipitation was estimated by the three kriging methods for the 478 DEM grid points by using the eight nearest neighbors within a radius of 60 km.

The optimum configuration for PRISM was also determined by jackknife cross validation, but did not require the initial selection of a model (it was prescribed as linear). PSTAT, a version of PRISM that calculates cross-validation residuals for point estimates, was used. PSTAT automatically varied three key input parameters: minimum and maximum radius of influence (MINRAD and MAXRAD) and the minimum number of stations sought for developing precipitation–DEM elevation functions (MINSTA). The model configuration that resulted in the lowest mean absolute error (MAE) and bias was chosen as the configuration for the application. MAE was given precedence if one configuration did not produce both the lowest MAE and bias. Bias was calculated as

$$\text{bias} = \frac{1}{n}\sum_{i=1}^{n}(P_i - O_i), \qquad (6)$$

where $P_i$ and $O_i$ are the predicted and observed precipitation for the $i$th station, respectively. MAE was defined as

TABLE 2. Values of input parameters for PRISM applications to the Willamette River basin, northern Oregon, and the western United States.

| Parameter | Willamette River basin | Northern Oregon | Western United States |
|---|---|---|---|
| MINSTP | 15 meters per grid cell | 15 meters per grid cell | 15 meters per grid cell |
| MAXRAD | 7 grid cells | 4 grid cells | 3 grid cells |
| MINRAD | 4 grid cells | 3 grid cells | 1 grid cell |
| MINSTA | 3 stations | 5 stations | 6 stations |
| BIMIN | 0.0 km | 0.0 $km^{-1}$ | 0.0 $km^{-1}$ |
| BIMAX | 3.0 $km^{-1}$ | 3.0 $km^{-1}$ | 3.0 $km^{-1}$ |
| DB1 | 0.8 $km^{-1}$ | 1.15 $km^{-1}$ | 0.97 $km^{-1}$ |
| B1EX | 2.0 $km^{-1}$ | 2.0 $km^{-1}$ | 2.0 $km^{-1}$ |
| BIMAXG | N/A* | 4.0 $km^{-1}$ | 4.0 $km^{-1}$ |
| MINSLP | N/A | 100 m | 100 m |

* N/A—the GRADIENT postprocessor was not needed in the Willamette Valley application.

$$\text{MAE} = \frac{1}{n} \sum_{i=1}^{n} |P_i - O_i|, \qquad (7)$$

and DB1 (the default precipitation–DEM elevation slope) was initialized at 0.9 $km^{-1}$, a typical value for the western United States. In PSTAT, MINRAD and MAXRAD were each varied from 2 to 10 grid cells (10′–50′ of latitude and longitude), and MINSTA was varied from 2 to 10 stations. The optimum configuration was MINRAD = 4 cells, MAXRAD = 7 cells, and MINSTA = 3 stations. A run of PRISM with these settings gave an average B1 over the modeling domain of 0.8. This value was then substituted for the initial DB1 and PSTAT run again to insure that the overall ranking of configurations did not change (it did not in this case). Table 2 lists values of all input parameters for the application.

For this application, PRISM calculated 478 regression functions, one for each DEM cell. Of these, the precipitation–DEM elevation slopes for 62 cells (13%) failed to fall within B1MIN and B1MAX after attempts at outlier deletion. Of the remaining regression lines, the mean $r^2$ (coefficient of determination) of those that used at least three stations was 0.64. This is similar to the $r^2$ of 0.67 for the domainwide regression between log annual precipitation and log elevation used in detrended kriging (Phillips et al. 1992).

PRISM exhibited the lowest cross-validation errors, followed by detrended kriging, cokriging, and kriging (Table 3). The bias for PRISM was 0.1 cm, compared to −1.4, −2.0, and −5.2 cm for detrended kriging, cokriging, and kriging, respectively. The MAE was 17 cm for PRISM, 19 cm for detrended kriging, 20 cm for cokriging, and 26 cm for kriging.

The precipitation field produced by detrended kriging, the geostatistical method with the best statistical performance, is shown in Fig. 6a. A general minimum in precipitation of about 90–100 cm occurred in the northern Willamette Valley. (The minimum estimate of 57 cm reported in Table 3 appears to have been caused by edge effects on the northern margin of the domain.) Smoothed, large-scale precipitation maxima were produced in the Coast Range and at middle elevations of the Cascades.

The PRISM precipitation field exhibited relatively detailed local patterns (Fig. 6b). The minimum estimate of 93 cm occurred northwest of Salem. The maximum estimate of 344 cm, 51 cm above the highest measured value, occurred on the slope of Mount Jefferson at the eastern edge of the domain. The field showed a rapid increase in precipitation on the western edge of the domain, which corresponds to the eastern slope of the Coast Range. Numerous local maxima occurred on the western slope of the Cascades, corresponding with minor mountain peaks; these maxima are largely missing from the detrended kriging field. Comparisons with the best available isohyetal map for Oregon (USDA Soil Conservation Service 1964), which provides substantial detail in mountainous areas, indicated that the precipitation field from PRISM corresponded more closely to the isohyetal map than did those from the geostatistical methods.

### *b. Northern Oregon*

PRISM was applied to northern Oregon to assess its performance in a region that encompasses several radically different orographic regimes and incorporates

TABLE 3. Summary statistics for precipitation estimates by PRISM, kriging, detrended kriging, and cokriging in the Williamette River basin.

| Method | Minimum estimate (cm) | Maximum estimate (cm) | Mean estimate (cm) | X-val* bias (cm) | Mean absolute X-val error (cm) |
|---|---|---|---|---|---|
| PRISM | 93 | 344 | 157 | 0.1 | 17 |
| Kriging | 102 | 265 | 157 | −5.2 | 26 |
| Detrended kriging | 57 | 259 | 170 | −1.4 | 19 |
| Cokriging | 60 | 319 | 167 | −2.0 | 20 |
| Station precipitation values ($n$ = 52) | 99 | 293 | 164 | — | — |

* Cross validation.

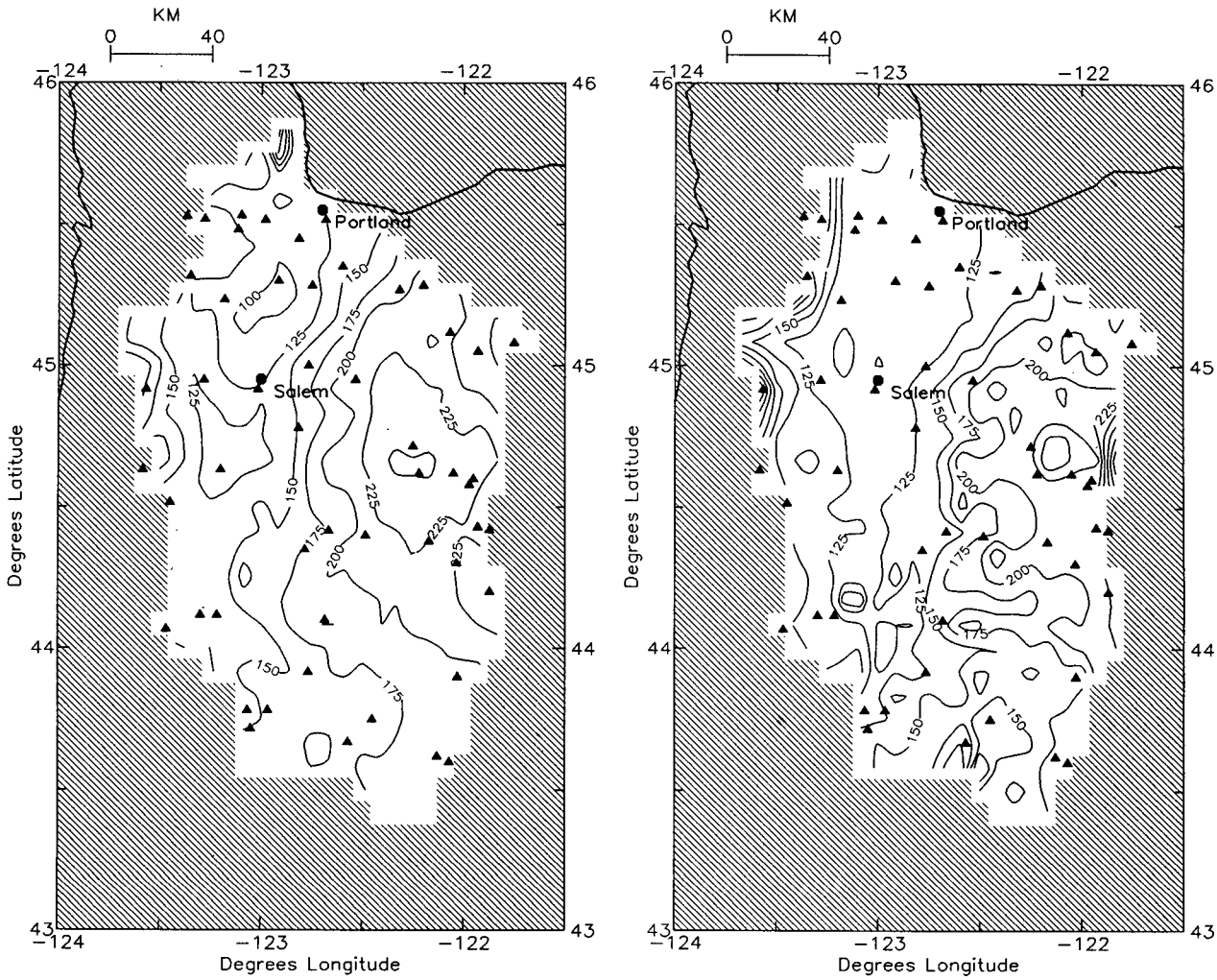


FIG. 6. Predicted annual precipitation fields for the Willamette River basin produced by (a) detrended kriging and (b) PRISM. Contour interval is 25 cm.

extreme spatial gradients in precipitation. The modeling domain extends eastward from the Pacific coast, across the Coast and Cascade ranges, to the Wallowa Mountains of northeastern Oregon; it spans southward from southern Washington to Bend, Oregon (Fig. 7). Measured annual precipitation in the domain ranges from less than 25 cm in the interior desert to over 325 cm in the Coast Range and northern Cascades—one of the greatest precipitation ranges in the United States for a region this size. A domainwide precipitation–elevation relationship is virtually nonexistent. Indeed, the lowest measured precipitation in the domain (Redmond, Oregon) is at 917 m above mean sea level (MSL) and the highest (North Fork, Oregon) is at 769 m MSL. The lack of a domainwide relationship between precipitation and elevation renders invalid any interpolation methods that rely on such relationships. It is for this reason that cokriging and elevation detrended kriging cannot be applied here, unless the domain is split up into many subregions and the interpolation done in a piecewise manner (Phillips et al. 1992).

The precipitation dataset for northern Oregon was a combination of 130 National Weather Service and cooperator stations (EarthInfo 1990) and 51 SNOTEL sites (USDA Soil Conservation Service 1988). To be included in the dataset, the National Weather Service stations must have had at least 20 years of record (regardless of the measurement period) and at least 75% data completion rate. All SNOTEL stations with valid 1961–85 average annual precipitation were included.

PRISM was applied for monthly and annual average precipitation. The values of MINRAD = 3 cells, MAXRAD = 4 cells, and MINSTA = 5 stations were used for all months, and were determined by running cross-validation statistics on the annual average precipitation with PSTAT. The values of all input parameters are listed in Table 2. To minimize edge effects,

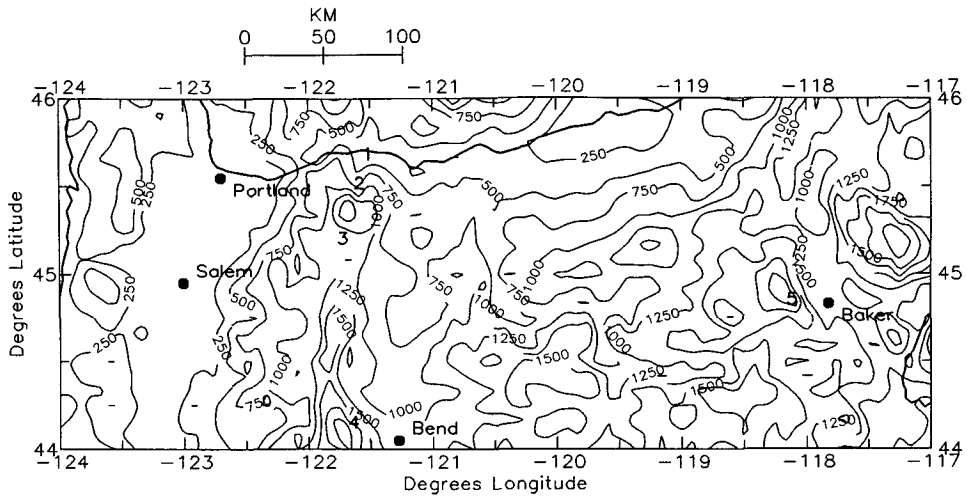


FIG. 7. Northern Oregon PRISM modeling domain. Elevation contour interval is 250 m. The numbers 1–5 indicate stations having observed annual precipitation that differed markedly from PRISM predictions in cross validation.

the model was originally applied for a domain that ranged from 43°–47°N to 116°–125°W—1° latitude and longitude beyond the domain shown in Fig. 7. The predicted grid was then taken as a window of the original, and performance was evaluated only for stations within this window. The windowed domain (Fig. 7) required 2016 regression functions for each month and for the year, for a total of 26 208 functions. Of these, 13%–18% had slopes that did not fall between B1MIN and B1MAX after attempts at outlier deletion.

Results from the PRISM application to northern Oregon are summarized in Tables 4 and 5. Table 4 compares performance statistics from the northern Oregon application to the Willamette River basin application. The minimum estimated annual value was 13 cm, 35% below the lowest measured value, and the maximum was 556 cm, 62% above the highest measured value (Table 4). Cross-validation bias was 1.3 cm, somewhat higher than the 0.1-cm bias for the Willamette River basin. The MAE was 17 cm, the same as that for the Willamette River basin. However, the average estimated precipitation was 56 cm lower in northern Oregon than in the Willamette River basin. Thus, errors expressed as a percentage of each observed value, and then averaged, were believed to be more comparable than absolute units. On a percentage basis, the bias increased from 1% to 4.5% and the MAE increased from 10% to 16%.

An examination of the annual cross-validation residuals revealed that 5 out of the 181 stations had particularly large residuals. They were 1) Hood River—133 cm predicted versus 75 cm observed; 2) Parkdale—

TABLE 4. Summary statistics for PRISM applications to the Willamette River basin, northern Oregon, and the western United States. Cross-validation bias and mean absolute error are expressed in centimeters and in percentage of observation. The percent value is arrived at by expressing each error as a percentage of the observation, then averaging them. All statistics are for average annual precipitation.

| Domain | Minimum estimate (cm) | Maximum estimate (cm) | Mean estimate (cm) | X-val* bias (cm)/(% obs) | Mean absolute X-val error (cm)/(% obs) |
|---|---|---|---|---|---|
| Willamette River basin PRISM | 93 | 344 | 157 | 0.1/1.0 | 17/10 |
| Northern Oregon PRISM | 13 | 556 | 101 | 1.3/4.5 | 17/16 |
| Northern Oregon station precipitation values ($n$ = 181) | 20 | 331 | 107 | — | — |
| Western U.S. PRISM | 0.1 | 923 | 51 | 1.5/3.5 | 9/17 |
| Western U.S. station precipitation values ($n$ = 3500) | 4 | 347 | 57 | — | — |

* Cross validation.

TABLE 5. Monthly and annual summary statistics for PRISM precipitation estimates for northern Oregon. Cross-validation bias and mean absolute error are expressed in centimeters and in percentage of observation. The percent value is arrived at by expressing each error as a percentage of the observation, then averaging them.

| Month | Mean $P/E$* regression $r^2$ | Mean precipitation (cm) | Mean regression slope ($km^{-1}$) | X-val** bias (% obs) | Mean absolute X-val error (% obs) |
|---|---|---|---|---|---|
| January | 0.61 | 14 | 1.2 | 6.7 | 22 |
| February | 0.61 | 11 | 1.3 | 8.0 | 25 |
| March | 0.63 | 10 | 1.2 | 5.8 | 21 |
| April | 0.63 | 6 | 1.1 | 4.5 | 20 |
| May | 0.65 | 5 | 1.1 | 5.0 | 19 |
| June | 0.64 | 4 | 1.1 | 5.5 | 18 |
| July | 0.55 | 1 | 1.0 | 8.0 | 27 |
| August | 0.56 | 2 | 1.0 | 7.0 | 25 |
| September | 0.64 | 4 | 1.1 | 4.4 | 21 |
| October | 0.65 | 7 | 1.2 | 5.6 | 21 |
| November | 0.68 | 14 | 1.2 | 6.2 | 21 |
| December | 0.67 | 16 | 1.2 | 7.2 | 22 |
| Annual | 0.70 | 101 | 1.2 | 4.5 | 16 |

* Precipitation–DEM elevation.
** Cross validation.

177 versus 103 cm; 3) Clear Lake—206 versus 122 cm; 4) Three Creeks Meadow—177 versus 111 cm; and 5) Eilertson Meadows—134 versus 77 cm. These stations are shown as bold numbers in Fig. 7. Stations 1–4 are located within steep precipitation gradients just to the east of the Cascade crest, and Eilertson Meadows is within a strong precipitation gradient between Baker, Oregon, and Rock Creek Butte, 35 km west of Baker. These steep gradients are areas of high spatial uncertainty in the prediction grid. For example, Three Creeks Meadow is a SNOTEL site located about 25 km northwest of Bend, on the eastern slope of the Three Sisters. The precipitation gradient from the PRISM prediction grid averaged 20 cm per horizontal kilometer across the site. Thus, the 72-cm overprediction by PRISM actually amounted to a spatial displacement error of less than 4 km.

All five of the above stations were overpredicted by PRISM. It may be that the change in precipitation with elevation is nonlinear in leeside areas, dropping off very steeply just below the crest and leveling off as distance from the crest increases. Or, the orographic scale in these situations may be less than that of the 5-min grid, and overprediction is being caused by a lack of spatial resolution. (The overpredictions cannot be attributed to the action of GRADIENT, because cross-validation is done totally within PSTAT.)

Contour plots of mean annual precipitation and prediction intervals as estimated by PRISM are shown in Fig. 8. The greatest estimated precipitation totals occurred in the Coast Range (Fig. 8a). Two areas, one west of Portland and one west of Salem, exceeded 450 cm. In comparison, the USDA Soil Conservation Service (1964) located the maximum precipitation areas in exactly the same places, and estimated that 350–500 cm fell annually in these locales. Sparse data (less than 3 stations per regression function) limited the estimation of prediction intervals in the Coast Range (Fig. 8b). Large areas showing prediction intervals of less than ±25% in the vicinity of Portland and Salem reflected greater data density in the Willamette Valley. In the Cascades, PRISM produced broad areas of precipitation above 200 cm, with maxima occurring on the high Cascade crests. Estimated peak precipitation on Mount Hood and the Three Sisters exceeded 300 cm, and Mount Jefferson exceeded 400 cm. The USDA Soil Conservation Service (1964) estimated maxima of 250–350 cm on these peaks. Prediction intervals (95%) ranged from ±25%–75% in the southern portion of the Cascades to ±50%–100% in the northern portion.

Precipitation east of the Cascades was estimated by PRISM to be comparatively light (Fig. 8a). Broad regions receiving less than 50 cm annually were common. Mountainous areas received locally higher amounts. The highest modeled precipitation total east of the Cascades was in the Wallowa Mountains on the eastern border of the modeling window. Here, over 250 cm was estimated on the highest peaks. The USDA Soil Conservation Service (1964) estimated that up to 200 cm fell in this region. Extremely low data density severely reduced the number of prediction interval estimates in eastern Oregon (Fig. 8b). Intervals were lowest in comparatively flat, populated areas along the Oregon–Washington border, north of Bend, and near Baker. Prediction intervals (95%) averaged about ±25% to ±75% in the Wallowa Mountains.

Summary statistics for the monthly PRISM predictions show a pronounced minimum in domainwide precipitation during the summer (Table 5). The lowest monthly mean regression coefficients and highest cross-validation bias and mean absolute error also occurred in summer. This appears to have been caused by the

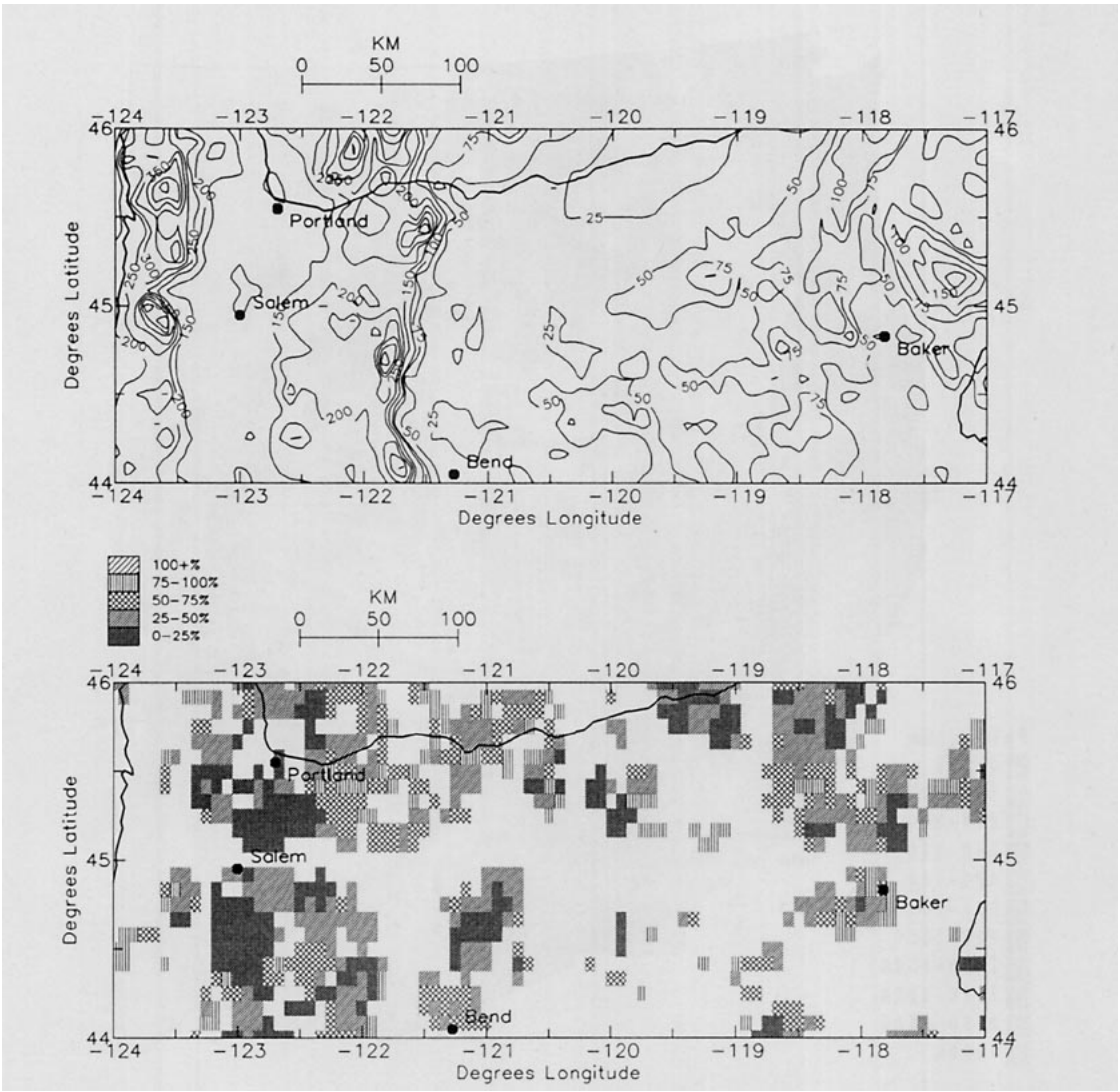


FIG. 8. Northern Oregon (a) annual precipitation and (b) 95% prediction half-intervals produced by PRISM. Contour interval for precipitation is 25 cm below 100 cm, and 50 cm above 100 cm. A prediction half-interval of 50% means there is a 95% probability that the actual precipitation is within 50% of the predicted value.

light and spatially complex nature of the summer precipitation in the region. Mean slopes of the regressions were fairly stable, when reported as a fraction of the average precipitation of the stations used in each regression. As was expected, monthly cross-validation errors were higher than annual errors. This is due to the greater variability and generally weaker precipitation–DEM elevation relationships of monthly precipitation compared to annual totals.

### c. *Western United States*

To assess the ability of PRISM to maintain predictive capability over very large, complex regions, the model was applied to an area bounded by 125° and 104°W (Pacific coast to slightly east of the Rocky Mountains) and 31° and 49°N (U.S.–Mexican border to the U.S.–Canadian border). Annual precipitation was predicted using 3091 National Weather Service and cooperator precipitation stations (EarthInfo 1990) and 423 SNOTEL stations (USDA Soil Conservation Service 1988); selection criteria were the same as for the northern Oregon application. Values of all input parameters are shown in Table 2. Summary statistics for the application are in Table 4. Cross-validation bias was 3.5%, compared to 4.5% in northern Oregon. Cross-validation MAE increased slightly, rising to 17% from 16% in northern Oregon.

Gridded annual average precipitation produced by PRISM for the western United States is shown in Fig. 9. PRISM captures regional trends in precipitation from wet coastal areas to interior deserts, as well as

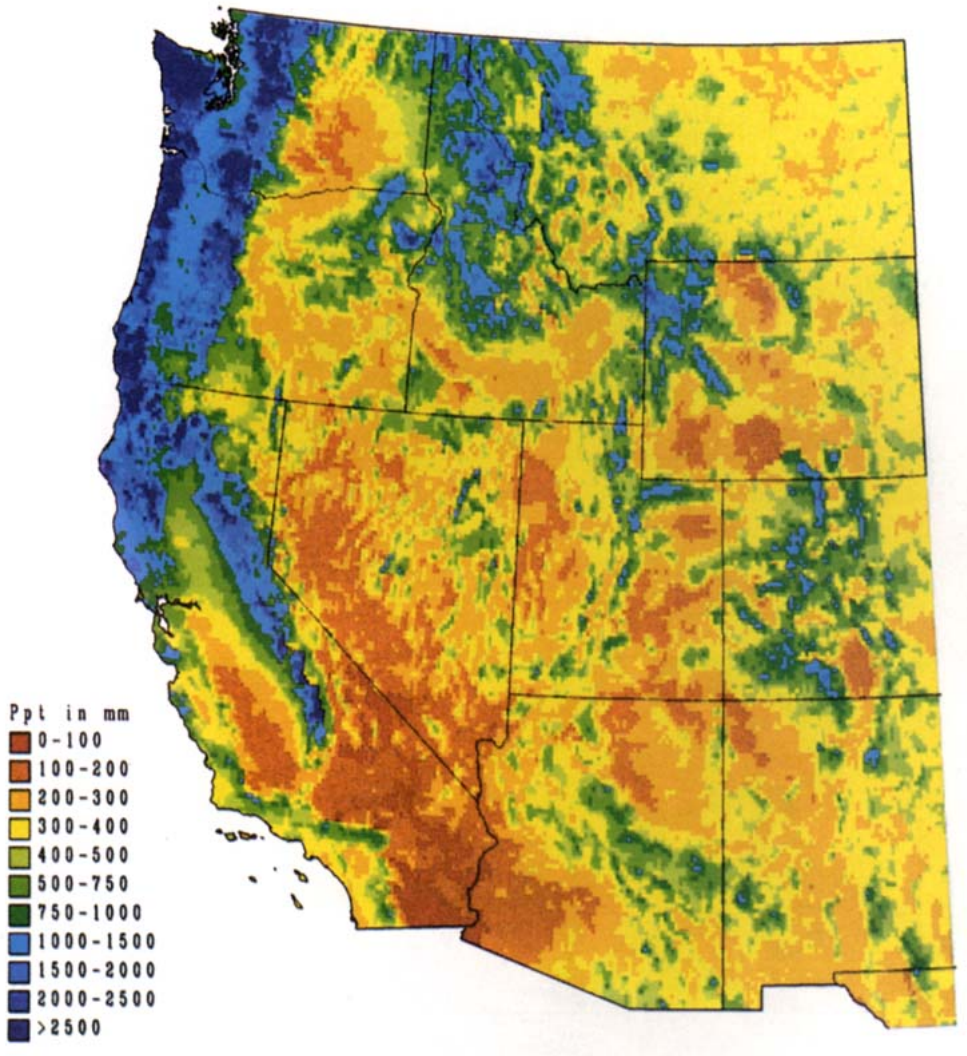


FIG. 9. Annual average precipitation for the western United States estimated by PRISM.

detailed patterns resulting from complex mountain and valley systems. PRISM reproduces the gentle increases in precipitation on the windward slopes of the Cascades and Sierra Nevada, as well as sharp decreases on the leeward sides of these ranges. Throughout the west, PRISM estimates what appear to be realistic precipitation values on many isolated peaks and ranges for which no data are available.

While PRISM accurately estimates precipitation for most areas, the estimates would undoubtedly improve if the model was applied to smaller subdomains with input parameters (i.e., MINRAD, MAXRAD, MAXSTA, etc.) set to reflect local conditions and data availability. In addition, the National Weather Service and SNOTEL data have not been subjected to rigorous checks for quality or accuracy. This may be an important factor in data-sparse regions such as Nevada, where each data point has an usually large influence on the estimated precipitation.

## 6. Summary and further work

The purpose of this study was to develop a method for distributing point measurements of monthly and annual average precipitation to regularly spaced grid cells at regional and continental scales. The main focus was on developing a conceptual framework for mapping orographic precipitation in complex terrain. The result was an objective precipitation distribution model called PRISM. PRISM brings a unique combination of climatological and statistical concepts to the mapping of orographic precipitation.

The PRISM modeling system was compared to commonly used geostatistical methods—kriging, detrended kriging, and cokriging. The four methods were applied to the Willamette River basin, Oregon, and evaluated by both quantitative and qualitative methods. PRISM exhibited superior performance in all categories. To assess its adaptability and flexibility, PRISM

was applied to northern Oregon and to the entire western United States. Detrended kriging and cokriging could not be used in these regions, because there was no overall relationship between elevation and precipitation. PRISM's statistical performance in northern Oregon deteriorated a small to moderate amount compared to its performance in the Willamette River basin. An application of PRISM to the western United States showed no further deterioration. Because PRISM continually adjusts its frame of reference by using localized precipitation–DEM elevation relationships, errors are apparently contained at low levels despite the number and diversity of orographic regimes operating within a region.

The ability of PRISM to maintain predictive accuracy over large areas makes it extremely useful for developing isohyetal maps for states or regions. PRISM was used to develop a new official isohyetal map for Oregon (Taylor 1993, personal communication). The model is currently being used to produce detailed precipitation maps of Idaho, Utah, and Nevada for the USDA Soil Conservation Service, and to produce a coarser isohyetal map of the contiguous United States for the U.S. Army Corps of Engineers. These PRISM analyses incorporate the latest station data with easy updating capabilities, and have the advantage of using an objective, reproducible, and GIS-compatible method that requires much less time and resources than a traditional manual analysis. The basic PRISM approach also appears promising for distributing other parameters that are locally correlated with elevation, such as temperature and snowfall.

The two most important limitations of this initial version of PRISM are 1) for regional applications in mountainous terrain, it performs consistently well only at DEM resolutions greater than about 6 km with routinely available data; and 2) there is a need to prescribe the slope of the precipitation–DEM elevation function to avoid underestimating precipitation on the upper slopes of some sharply defined mountains. Limitation 2 appears to be a side effect of using a coarse-grid DEM, which oversmoothes the elevations of sharply defined peaks. Limitation 2 would probably cease to be a problem if limitation 1 could be overcome—successfully running PRISM regionally at finer DEM resolutions. However, as was discussed in section 3b, arriving at an "optimal" DEM resolution presents a difficult problem of scale matching. At issue are the interrelationships between the hierarchy of orographic scales that may be present in a given region and the limitations placed on the analysis by the spatial (and temporal) scales of the available data. PRISM currently matches the spatial scale of its predictions to that of the data by generating topographic facet grids from lightly or heavily filtered DEMs as appropriate. This method is effective, except that the filtering procedure does not produce facet grids that represent a sufficiently wide range of scales. We are currently experimenting with a Gaussian filter that can reproduce an unlimited number of effective grid scales. This method may allow PRISM to be used with much finer resolution DEMs (e.g., 2 km), even if the available data typically can only resolve orographic effects at scales of 6 km and greater.

The model assumption that precipitation increases to a maximum at the crest of a local topographic barrier is generally applicable to the midlatitudes, but the exceptions discussed in section 3 should not be overlooked. Work to evaluate and possibly refine the assumption should be carried out by analyzing streamflow measurements from high mountain watersheds, assessing results from orographic precipitation modeling, and exploring the roles of gauge undercatch and other data quality issues in the underestimation of precipitation at high elevations.

As indicated in the title of this paper, PRISM estimates the spatial distribution of "climatological" precipitation in mountainous terrain. This assumes that precipitation has accumulated over enough storm events to produce a usable precipitation–elevation relationship. The minimum averaging period to qualify as "climatological" depends on storm type, seasonality, precipitation amount and variability, and a host of other factors. PRISM is being tested at time scales ranging from daily to annual in various seasons and locations to help characterize the minimum temporal scale at which the assumption of a usable precipitation–elevation relationship holds.

*Acknowledgments.* The authors wish to thank George H. Taylor and Wayne P. Gibson for their ongoing conceptual and technical contributions to PRISM, and E. George Robison and two anonymous reviewers whose suggestions helped produce a substantially better manuscript. The information in this article has been funded by the U.S. Environmental Protection Agency. This document has been prepared at the EPA Environmental Research Laboratory in Corvallis, Oregon, through Cooperative Agreement CR816257 with Oregon State University. It has been subjected to the agency's peer and administrative review, and it has been approved for publication as an EPA document. Mention of trade names or commercial products does not constitute endorsement of recommendation for use.

## REFERENCES

Alter, J. C., 1919: Normal precipitation in Utah. *Mon. Wea. Rev.*, **47**, 633–636.

Armstrong, C. F., and C. K. Stidd, 1967: A moisture-balance profile on the Sierra Nevada. *J. Hydrol.*, **5**, 258–268.

Barrows, H. K., 1933: Precipitation and runoff and altitude relations for Connecticut River. *Trans. Am. Geophys. Union*, **14**, 396–406.

Barry, R. G., 1973: A climatological transect on the east slope of the Colorado Front Range. *Arc. Alp. Res.*, **5**, 89–110.

——, and R. J. Chorley, 1976: *Atmosphere, Weather and Climate.* 3d ed. Methuen, 432 pp.

Bergeron, T., 1968: Studies of the oreigenic effect on the areal fine structure of rainfall distribution. Meteorological Institute, Uppsala Univ., Uppsala, Sweden, Report No. 6.

Burns, J. I., 1953: Small-scale topographic effects on precipitation distribution in San Dimas Experimental Forest. *Trans. Am. Geophys. Union,* **34,** 761–768.

Changnon, S. A., Jr., D. M. A. Jones, and F. A. Huff, 1975: Precipitation increases in the low hills of southern Illinois: Part 2. Field investigation of anomaly. *Mon. Wea. Rev.,* **103,** 830–836.

Chua, S-H., and R. L. Bras, 1982: Optimal estimators of mean areal precipitation in regions of orographic influence. *J. Hydrol.,* **57,** 23–48.

Dingman, S. L., D. M. Seely-Reynolds, and R. C. Reynolds III, 1988: Application of kriging to estimate mean annual precipitation in a region of orographic influence. *Water Resour. Bull.,* **24,** 329–339.

Dolph, J., D. Marks, and G. King, 1992: Sensitivity of the regional water balance in the Columbia River basin to climate variability: Application of a spatially distributed water balance model. *Watershed Management: Balancing Sustainability and Environmental Change,* R. J. Naiman, Ed., Springer-Verlag, 233–265.

Donley, D. E., and R. L. Mitchell, 1939: The relation of rainfall to elevation in the southern Appalachian region. *Trans. Am. Geophys. Union,* **20,** 711–721.

EarthInfo, Inc., 1990: *Climate Data User's Manual, TD3200 Summary of the Day—Cooperative Observer Network.* EarthInfo, Inc., 25 pp.

Fan, Y., and C. J. Duffy, 1991: Estimating space–time precipitation and temperature fields in mountainous terrain: Wasatch Range, Utah. *American Geophysical Union Fall Meeting Program and Abstracts,* San Francisco, CA., Amer. Geophys. Union.

Gjorsvik, O. G., 1972: Deficiencies in measured snow precipitation in a mountainous area in Norway. *Distribution of Precipitation in Mountainous Areas,* WMO Pub. 326(2), World Meteorological Organization, Geneva, 466–473.

Hanson, C. L., R. P. Morris, R. L. Engleman, D. L. Coon, and C. W. Johnson, 1980: Spatial and seasonal precipitation distribution in southwest Idaho. *Agricultural Reviews and Manuals, ARM-W-13,* USDA Dept. of Agriculture, Science and Education Administration, 15 pp.

Hart, F. C., 1937: Precipitation and run-off in relation to altitude in the Rocky Mountain region. *J. Forestry,* **35,** 1005–1010.

Hay, L. E., M. D. Branson, and G. H. Leavesly, 1991: The effects of scale on precipitation estimates from an orographic precipitation model. *American Geophysical Union Fall Meeting Program and Abstracts,* San Francisco, CA.

Henry, A. J., 1919: Increase of precipitation with altitude. *Mon. Wea. Rev.,* **47,** 33–41.

Hevesi, J. A., J. D. Istok, and A. L. Flint, 1992a: Precipitation estimation in mountainous terrain using multivariate geostatistics. Part I: Structural analysis. *J. Appl. Meteor.,* **31,** 661–676.

——, A. L. Flint, and J. D. Istok, 1992b: Precipitation estimation in mountainous terrain using multivariate geostatistics. Part II: Isohyetal maps. *J. Appl. Meteor.,* **31,** 677–688.

Hibbert, A. R., 1977: Distribution of precipitation on rugged terrain in central Arizona. *Hydrol. Water Resour. Ariz. Southwest,* **7,** 163–173.

Houghton, J. G., 1979: A model for orographic precipitation in the north-central Great Basin. *Mon. Wea. Rev.,* **107,** 1462–1475.

Hutchinson, P., 1968: An analysis of the effect of topography on rainfall in the Taieri Catchment area, Otago. *Earth Sci. J.,* **2,** 51–68.

Lee, C. H., 1941: Total evaporation from Sierra Nevada watersheds by the method of precipitation and runoff differences. *Trans. Am. Geophys. Union,* **22,** 50–66.

Longley, R. W., 1975: Precipitation in valleys. *Weather,* **30,** 294–300.

Lull, H. W., and L. Ellison, 1950: Precipitation in relation to altitude in central Utah. *Ecology,* **31,** 479–484.

Marwitz, J. D., 1987: Deep orographic storms over the Sierra Nevada. Part I: Thermodynamic and kinematic structure. *J. Atmos. Sci.,* **44,** 159–173.

Matheron, G., 1971: *The Theory of Regionalized Variables and its Applications.* Cahiers du Centre de Morphologie Mathematique, Ecole des Mines, 211 pp.

National Geophysical Data Center, 1989: *Geophysics of North America: User's Guide.* National Oceanic and Atmospheric Administration, U.S. Department of Commerce, 85 pp.

Neter, J., W. Wasserman, and M. H. Kutner, 1989: *Applied Linear Regression Models.* 2d ed. Richard D. Irwin, Inc., 667 pp.

Osborn, H. B., 1984: Estimating precipitation in mountainous regions. *J. Hydraul. Eng.,* **110,** 1859–1863.

Peck, E. L., and M. J. Brown, 1962: An approach to the development of isohyetal maps for mountainous areas. *J. Geophys. Res.,* **67,** 681–694.

——, and J. C. Schaake, 1990: Network design for water supply forecasting in the West. *Wat. Resour. Bull.,* **26,** 87–99.

Phillips, D. L., J. Dolph, and D. Marks, 1992: A comparison of geostatistical procedures for spatial analysis of precipitation in mountainous terrain. *Agric. For. Meteor.,* **58,** 119–141.

Rechard, P. A., 1972: Winter precipitation gage catch in windy mountainous areas. Distribution of Precipitation in Mountainous Areas, WMO Pub. 326(2), World Meteorological Organization, Geneva, 13–26.

Reed, W. G., and J. B. Kincer, 1917: The preparation of precipitation charts. *Mon. Wea. Rev.,* **45,** 233–235.

Rodda, J. C., and S. W. Smith, 1986: The significance of the systematic error in rainfall measurement for assessing wet deposition. *Atmos. Environ.,* **20,** 1059–1064.

Running, S. W., R. R. Nemani, and R. D. Hungerford, 1987: Extrapolation of synoptic meteorological data in mountainous terrain and its use for simulating forest evapotranspiration and photosynthesis. *Can. J. For. Res.,* **17,** 472–483.

Schermerhorn, V. P., 1967: Relations between topography and annual precipitation in western Oregon and Washington. *Water Resour. Res.,* **3,** 707–711.

Sevruk, B., 1974: The use of stereo, horizontal, and ground level orifice gages to determine a rainfall-elevation relationship. *Water Resour. Res.,* **10,** 1138–1141.

Smith, R. B., 1979: The influence of mountains on the atmosphere. Vol. 21, *Advances in Geophysics,* Academic Press, 87–230.

Spreen, W. C., 1947: A determination of the effect of topography upon precipitation. *Trans. Am. Geophys. Union,* **28,** 285–290.

Thiessen, A. H., 1911: Precipitation averages for large areas. *Mon. Wea. Rev.,* **39,** 1082–1084.

USDA Soil Conservation Service, 1964: *Normal Annual Precipitation 1930–1957, State of Oregon.* Weather Bureau River Forecast Center.

——, 1988: *Snow Survey and Water Supply Products Reference,* West National Technical Center, Snow Survey Program, 12 pp.

Varney, B. M., 1920: Monthly variations of the precipitation–altitude relation in the central Sierra Nevada of California. *Mon. Wea. Rev.,* **48,** 648–649.

Vuglinski, V. S., 1972: Methods for the study of laws for the distribution of precipitation in medium-high mountains (illustrated by the Vitim River basin). *Distribution of Precipitation in Mountainous Areas,* WMO Pub. 326(2), World Meteorological Organization, Geneva, 212–221.

Yates, S. R., and A. W. Warrick, 1987: Estimating soil water content using cokriging. *Soil Sci. Soc. Am. J.,* **51,** 23–30.